Anomalous Ion Heating in Lower Hybrid Wave Sustained Plasmas on the TST-2 Spherical Tokamak Device

Kotaro IWASAKI, Akira EJIRI, Naoto TSUJII, Kouji SHINOHARA, Osamu WATANABE, Seowon JANG, Yi PENG, Yuting LIN, Fumiya ADACHI and Tian YIMING

The University of Tokyo, Kashiwa 277-8561, Japan

(Received 10 May 2023 / Accepted 27 October 2023)

Power flow is important to understand the lower hybrid wave (LHW) sustained plasmas in the TST-2 spherical tokamak device. During LHW power modulation experiments responses of ion temperature were found. The ion temperature increased at the edge region during ON phases of LHW power, while the ion temperature was kept constant at the central region. A 0-dimensional power balance at a steady state was investigated, and it was found that the collisional ion heating by bulk electrons is about two orders of magnitude smaller than the charge exchange loss and the neoclassical transport loss. The results indicate anomalous ion heating by additional unidentified heating mechanism. The estimated additional heating power itself is much smaller than the LHW power, but there are several ambiguities in the estimation, and a further study is necessary.

Keywords: spherical tokamak, lower hybrid wave, ion heating

DOI: 10.1585/pfr.18.1402089

1. Introduction

Non-inductive current drive is essential for a spherical tokamak reactor, because it has little space for a large flux center solenoid which inductively drives the current. Lower hybrid wave current drive is one of the most efficient non-inductive current drive methods in conventional tokamaks, but a high efficiency was not demonstrated in spherical tokamaks so far. On the TST-2 spherical tokamak device, non-inductive start-up using lower hybrid wave (LHW) has been studied. The current drive efficiency has been improved by developing various LHW antennas [1–3], and plasma currents up to 27 kA, which is about 1/4 of the inductive plasma current, was achieved [4]. There seems to be, however, several power loss mechanisms deteriorating the current drive efficiencies [5–7]. One possibility, which has not been studied in detail, is the power flow from LHW to ions. LHW is believed to heat electrons due to its fast phase velocity, and no direct ion heating is expected. However, the ion temperature increase of up to about 10 eV was observed [8], though the neoclassical transport loss and the charge exchange loss can be large due to the low plasma current and the low electron density, respectively, and the collisional heating is small due to the low electron density. Thus, it is important to estimate the power flow to ions to see whether the power is non-negligible compared to the LHW power. In this paper we will presents the ion temperature measurement results and estimate the power balance of ions.

The paper is organized as follows. In Sec. 2, the ion temperature measurement during power modulation experiments with LHW is shown, and the ion power balance is estimated. In Sec. 3, possibility of the ion heating by parametric decay instability (PDI) is discussed. Conclusion is given in Sec. 4.

2. LHW Power Modulation Experiments

TST-2 is a spherical tokamak located at the University of Tokyo (a typical major radius of the magnetic axis is 0.36 m, a minor radius is 0.23 m, the maximum toroidal field strength is 0.3 T) [9]. Capacitively coupled combline antennas are installed at outer-midplane [3] and top [10] to study different current drive scenarios using LHW [11] with $N_{\parallel} = 5.5$ and $N_{\parallel} = 4.9$ respectively, where $N_{\parallel}$ is the normalized parallel wave number of the launched wave. The source power is up to about 100 kW for each antenna. A visible spectrometer with one spatial viewing chord was used to measure the ion temperature from the CIII (464.74 nm, C^{2+}) line. Eight tangential radii were measured by changing the sight-line shot by shot.

Figure 1 shows typical waveforms of an LHW power modulation experiment. The top launched antenna was mainly used for driving current, but at initial plasma current was driven by the outer midplane antenna, up to 6 kA in this case. Before the start of modulation, the plasma had the following parameters: plasma current $I_p = 15$ kA, line integrated density $n_e l = 1.0 \times 10^{17}$ m^{-2}, toroidal field $B_t = 0.15$ T (at $R = 0.38$ m), launched LHW power $P_{LH} = 60$ kW. The modulation period was 6 ms. Figure 2 shows the profiles of the electron density and the temperature at 60 ms measured by a Thomson scattering sys-

author's e-mail: iwasaki@fusion.k.u-tokyo.ac.jp

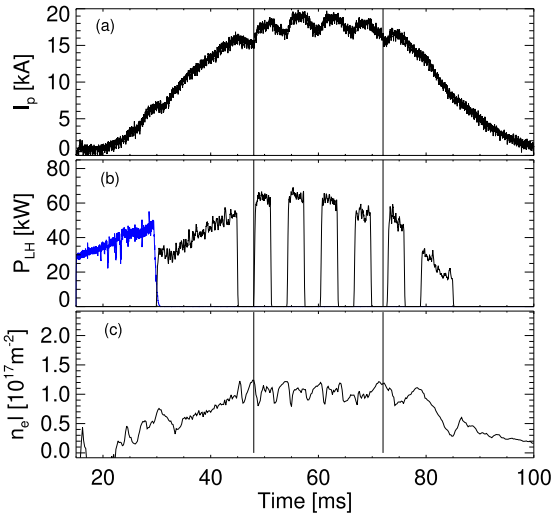

Fig. 1 Waveforms of plasma current I_p (a), net LH power P_{LH} (b) and line-integrated density $n_e l$ (c). Plasma current was mainly driven by top launch antenna (black), but initially driven by outer midplane launched antenna (blue). The vertical solid lines indicate the time window of our analysis.

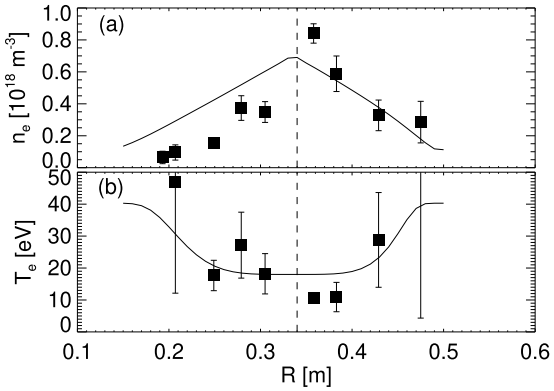

Fig. 2 Electron density n_e (a) and temperature T_e (b) profiles measured at 60 ms by the thomson scattering. The dashed line indicates the position of magnetic axis.

tem [12, 13]. The electron density shows a peaked profile ($n_e < 1 \times 10^{18}$ m^{-3}) while the temperature shows a hollow profile (about 20 eV at the center of $R = 0.34$ m and about 40 eV at the edge of $R = 0.15, 0.50$ m.). After turning off the LHW, the electron density and the temperature did not change in the central region within error bars, while the edge density showed a small change and the edge electron temperature showed a decrease. During the time period of 48 - 72 ms (indicated by the two vertical lines in Fig. 1), the plasma position, size, density were almost constants, and the data during that time period is analyzed. Since the light emission from LHW plasma is weak especially in the edge region due to the low density, the four modulation cycle averaged values are analyzed. A cycle is divided into 6 sections (1 ms for 1 section), and the two sections

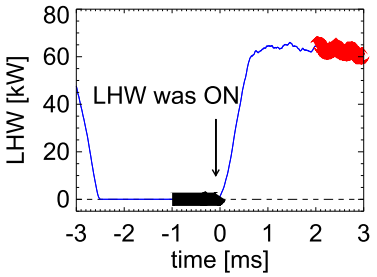

Fig. 3 The diagram which shows the phase of calculated. A thick black line indicates OFF-, a thick red line indicates ON-phases used in the analysis.

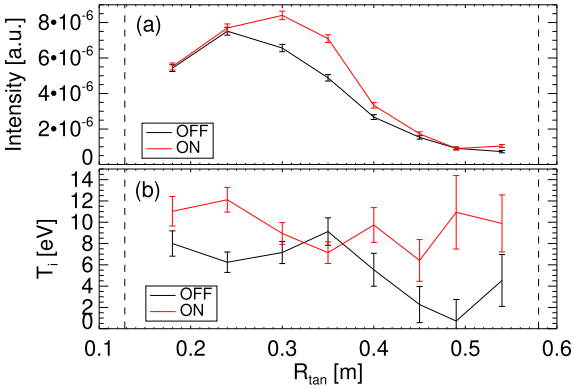

Fig. 4 Intensity of C III (a) and Ion temperature T_i (b) versus tangent radius of line of sight R_{tan}. A black line shows the ion temperature on OFF phase and a red line shows that on ON phase. Dashed lines show limiter positions.

are selected for the following analysis of ion temperature. The two sections are the OFF- and ON-phases shown in Fig. 3, The ion temperature profiles were obtained by using 8 reproducible discharges with 8 different lines of sight. The obtained profiles is shown in Fig. 4. The intensity of C III is a function of electron density, electron temperature, and impurity density. The change in intensity was smaller than the change in the the edge ion temperature, indicating that the electron density, electron temperature and impurity density didn't vary significantly. It should be noted that the monotonic intensity decrease at $R_{tan} > 0.3$ m (Fig. 4 (a)) indicates that line integration effect is not serious and $T_i(R_{tan}) \approx T_i(R)$ at $R_{tan} > 0.3$ m. At $R_{tan} > 0.3$ m the contribution of the intensity at $R \sim R_{tan}$ dominates the line-integrated signal, while at $R_{tan} < 0.3$ m contributions from other regions can be comparable. After LHW was ON, the edge ion temperature increases, while the central temperature does not change. The profile becomes flat and averaged temperature is about 10 eV. After LHW power is OFF, the time-reversed behaviors were observed. The large edge ion temperature response and the small central ion temperature response indicate that ion heating occurs at the edge region. Since LHW is believed to heat electrons, not ions since the large difference between the phase

velocity of the wave and thermal velocity of ions due to their large mass, one possible ion heating mechanism is the collisional ion heating by bulk electrons. Here, we calculate the steady-state power balance of ions during the ON-phase, in which the ion temperature shows a flat profile (10 eV) (see Fig. 4 (b)). The deuterium ion temperature and the measured C^{2+} ion temperature are considered to be the same, because the temperature relaxation time between D^+ and C^{2+} is about 0.07 ms, and this is much shorter than the energy confinement time which is estimated later.

For simplicity, we evaluate the 0-dimensional power balance between the four terms: collisional heating by electrons ($P_{\rm coll}$), charge exchange loss ($P_{\rm cx}$), transport loss ($P_{\rm transport}$), and an additional heating term ($P_{\rm add}$) determined to satisfy the power balance. That is, we evaluate $0 = P_{\rm coll} + P_{\rm cx} + P_{\rm transport} + P_{\rm add}$. The following values are used to evaluate the collisional heating; the electron temperature $T_{\rm e}$ is 18 eV at the center and 40 eV at the edge, the densities $n_{\rm e} = n_{\rm i}$ are $7 \times 10^{17}\,{\rm m}^{-3}$ at the magnetic axis and $1 \times 10^{17}\,{\rm m}^{-3}$ at the edge (shown by black curves in Fig. 2), and the ion temperature $T_{\rm i}$ is 10 eV, and then $P_{\rm coll} = \int (3/2) n (T_{\rm e} - T_{\rm i})/\tau_{\rm ei} dV = +35$ W, where $\tau_{\rm ei}$ is the heat exchange time between electrons and ions [14]. The charge exchange loss is evaluated by $P_{\rm cx} = -(3/2) n_{\rm i} n_0 (T_{\rm i} - T_0) S_{\rm cx} V$, where $n_{\rm i}$ is the (deuterium) ion density, n_0 is the neutral density, T_0 is the the neutral temperature, V is the plasma volume and $S_{\rm cx}$ is the rate coefficient for charge exchange per atom, $S_{\rm cx} = 1.066 \times 10^{-14} T_i^{0.327}$ [15]. Due to the low electron density, the neutrals can fully penetrate through the plasma, and n_0 inside the vacuum vessel is probably uniform. During the discharge, a nude gauge indicated that the pressure in the vacuum vessel was about 3×10^{-5} Torr, while the filling pressure was 9×10^{-5} Torr. Since the time response of the gauge was not so fast, the actual pressure may be lower than this. According to Ref. [16], the pressure in the LATE device decreased to about 1/10 of the initial pressure. Thus we adopt 1/10 of the filling pressure (9×10^{-6} Torr) to estimate n_0, and this would probably provide the lower limit of n_0 ($=3 \times 10^{17}\,{\rm m}^{-3}$). For $T_{\rm i} = 10$ eV, $T_0 = 4$ eV, $n_{\rm i} = 5 \times 10^{17}\,{\rm m}^{-3}$ and $V = 0.4\,{\rm m}^3$, the charge exchange loss calculated by the above equation is $P_{\rm cx} \sim -2000 \pm 1000$ W. Here we adopt $T_0 = 4$ eV considering Franck-Condon atoms [17] to estimate the lower limit. The transport loss is estimated using the neoclassical theory. In this experiment's parameters, the diffusion coefficient in the edge plasma is in a banana region, and the heat diffusion coefficient is written as $\chi_{\rm neo} = (R/a)^{3/2} q^2 \rho_{\rm i} \nu_{\rm ii}$ (Eq. (7.26) in [18]), where R is the major radius, a is the minor radius, q is the safety factor, $\rho_{\rm i}$ is the ion larmor radius and $\nu_{\rm ii}$ is the collisional time between ions. Using the values: $R = 0.34$ m, $a = 0.2$ m, $q = 20$, $n_{\rm i} = 1 \times 10^{17}\,{\rm m}^{-3}$ and $T_{\rm i} = 10$ eV, $\chi_{neo} = 30\,{\rm m}^2/{\rm s}$. Assuming a 0th-order-Bessel function shape for the profile and a constant heat diffusion coefficient, the global energy confinement time can be expressed as $\tau_E = 0.26 a^2/\chi_{\rm neo} = 0.4$ ms [18]. The transport loss is $P_{\rm transport} = -(3/2) n_{\rm i} V T_i/\tau_E \sim -1000 \pm 600$, where the averaged ion density $n_{\rm i}$ is set to be $5 \times 10^{17}\,{\rm m}^{-3}$. Considering the above powers and the power balance, the additional heating term becomes $P_{\rm add} \sim +3000 \pm 1000$ W ($\gg P_{\rm coll}$). In order to estimate the errors of power, we adopt 50% for the parameters, such as n_0,$\tau_{\rm E}$, which have large uncertainties and large effects on the power estimations. Thus, we can conclude that the contribution of the collisional power transfer is too small to explain the measured ion temperature. Thus, the observed increase of the ion temperature is "anomalous". We have to find the mechanism to explain this anomalous heating. Here, we use the neoclassical theory for estimating the transport power loss, but the transport is anomalous in normal, and the loss power by the transport increases. As a result, the required additional power should be larger, which reinforces the above conclusion. It should be noted that $P_{\rm add}$ is much smaller than the net LHW power of 60 kW.

In the OFF-phase, we can explain the power balance as follows. We use the same values used for the ON-phase, except for the ion temperature. For $P_{\rm coll}$, the ion temperature profiles are changed, 9 eV at the center and 0 eV at the edge as shown in Fig. 4 (b) and $P_{\rm coll} = +45$ W. For $P_{\rm transport}$, the volume averaged ion temperature gets about 2 eV, and then $P_{\rm transport} = -570$ W. For $P_{\rm cx}$, the Frank-Condon atoms temperature (4 eV) is higher than the volume averaged ion temperature (2 eV), and then $P_{\rm cx}$ can be positive and $P_{\rm cx} = +410$ W. Finally, we obtain $P_{\rm add} \sim +100 \pm 500$ W, and this is much smaller than $P_{\rm add} \sim +3000 \pm 1000$ W in the ON-phase. This result does not deny the heating power other than $P_{\rm coll}$ (or $P_{\rm cx}$) in OFF-phase, but the existence of $P_{\rm add}$ is not much obvious compared with that of the ON-phase.

3. Discussion

The power fed to the antenna is about 60 kW and the transmission power which implies that most of the injected power is consumed around the antenna. The resistive loss at the antenna is small because of the impedance matched design. According to numerical simulations and past studies [5, 10, 11], the major part of the power is believed to be deposited to electrons making fast electrons, and most of the power to the fast electrons is lost by RF induced transport process and some of the power is used to heat bulk electrons. Besides the power to electrons, we should consider several processes which were not considered in those past studies. One is the power deposition at the SOL layer indicated by high energy electrons observed by electrostatic probes [7], and the other is the power to PDIs [6]. Further studies are necessary to understand the whole power flow in the LHW sustained plasmas.

Although the estimated (ion) confinement time is much shorter than a half of the modulation period (3 ms), the electron and ion temperature at the center region kept nearly constant during OFF-phase. It is possible for the

electrons to be heated by fast electrons with relatively low energies (from a few hundreds eV to 1 keV) [5, 11]. For the ions, the profile was flat in the ON-phase, and the edge ion temperature quickly decreases with the time scale of 0.5 ms after a turn-off of the power. The positive P_{CX} during the OFF-phase can mitigate the quick T_i decrease. The different behavior between the central and edge regions suggests that they are decoupled in heat transport, which could be induced by the difference in transport coefficient.

In the 0-dimensional calculations, we neglect the radiation power because it is negligibly small. The visible spectrum shows that H/D Balmer lines, CIII and OII lines are dominant lines in visible, and we cannot observe higher ionization stage C and O in the discharges analyzed in this paper. Note that we observe CV, OV in lines (in UV range) in high T_e ohmic discharge plasmas. The other impurity lines we can observe is CuI and MoI, which are the material of antenna coating and limiters. These suggest that the impurity radiation in shorter wavelength region is not significant. Past analysis using a wide range (200 - 800 nm) spectrometer shows that the radiation power in this region is less than 100 W, and it was concluded that the radiation did not affect the power balance.

An ion heating mechanism other than collisions with electrons is necessary. Wave heating is one possibility, but we need other waves, because LHW cannot resonate with ions. In TST-2, PDIs were frequently observed [6, 19, 20]. The LHW can decay into two daughter waves due to nonlinear wave interactions, one of which is the ion cyclotron quasi-mode (ICQM). ICQM damps quickly by ions. This leads to the ion heating. Ion heating by ICQM was reported in [21], in which the pump wave frequency was close to the cyclotron frequency and ion heating was associated with ion quasi-mode excitation. PDI can be the candidate heating mechanism, because the location where the ICQM is excited corresponds to the location of the temperature increase of ions. It is reported that PDI occur at the edge region or near the antenna in other devices [22, 23]. In TST-2, the R position of PDI occurrence estimated in [6] corresponds to the near antenna positions, and hence we can expect edge ion heating by PDIs. PDI measured on TST-2 is a non-resonant type and then the decay waves cannot exist without the pump LHW. This can explain the response to the LHW power modulation (Fig. 4 (b)).

4. Conclusion

In this study, LHW power modulation experiments were conducted to measure the ion temperature response to LHW power. The ion temperature profile was measured. A response of the ion temperature was observed only in the edge region, whereas the central temperature is constant within error bars. Thus, ion heating occurred in the edge region. A 0-dimensional steady state power balance analysis was performed to investigate the ion heating mechanism. It was found that the collisional ion heating by bulk electrons is about two orders of magnitude smaller than the charge exchange loss and the neoclassical transport loss. This indicates that the observed increase of the ion temperature is anomalous. The estimated unidentified ion heating power is about 3 kW, while the net LHW power is 60 kW. Thus, the power flow to ion does not affect the current drive scenario in TST-2. One possibility to explain the heating is that due to the PDI daughter waves, but further studies are needed to confirm the correlation between ion heating and PDI. This is our future work. It should be noted that the PDIs themselves can deteriorate the current drive efficiency even though the power flow to ions is negligible.

Acknowledgments

This work was supported by JSPS KAKENHI Grant Numbers 22K03573, 18K13524 and 21226021, NIFS Collaboration Research Programs NIFS18KOAR22 and NIFS20KUTR155 and Japan/US Cooperation in Fusion Research and Development.

[1] Y. Takase *et al.*, Nucl. Fusion **51**, 063017 (2011).
[2] T. Wakatsuki *et al.*, Nucl. Fusion **54**, 093014 (2014).
[3] T. Shinya *et al.*, Nucl. Fusion **55**, 073003 (2015).
[4] S. Yajima *et al.*, Plasma Fusion Res. **13**, 3402114 (2018).
[5] A. Ejiri *et al.*, Plasma Fusion Res. **17**, 1402037 (2022).
[6] Y. Ko *et al.*, Plasma Fusion Res. **15**, 2402007 (2020).
[7] J.H.P. Rice *et al.*, Plasma Fusion Res. **15**, 2402009 (2020).
[8] S. Tsuda *et al.*, Plasma Fusion Res. **10**, 1202064 (2015).
[9] Y. Takase *et al.*, Nucl. Fusion **41**, 1543 (2001).
[10] S. Yajima *et al.*, Nucl. Fusion **59**, 066004 (2019).
[11] N. Tsujii *et al.*, Nucl. Fusion **57**, 126032 (2017).
[12] H. Togashi *et al.*, Plasma Fusion Res. **10**, 1202082 (2015).
[13] H. Togashi *et al.*, JINST **10**, 12020 (2015).
[14] e.g. J. Wesson, *Tokamaks* (Clarendon Press, Oxford, 2004).
[15] B. Lloyd *et al.*, Plasma Phys. Control. Fusion **38**, 1627 (1996).
[16] T. Yoshinaga *et al.*, Plasma Fusion Res. **81**, 333 (2005).
[17] J. Huang *et al.*, Nucl. Fusion **46**, 262 (2006).
[18] K. Miyamoto, *Fundamentals of Plasma Physics and controlled Fusion* (NIFS-PROC-48, National Institute for Fusion Science, 2000).
[19] Y. Adachi *et al.*, Rev. Sci. Instrum. **79**, 10F507 (2008).
[20] T. Oosako *et al.*, Nucl. Fusion **49**, 065020 (2009).
[21] M. Ono *et al.*, Phys. Fluids **23**, 1675 (1980).
[22] S.G. Beak *et al.*, Phys. Plasmas **21**, 061511 (2014).
[23] B.J. Ding *et al.*, Nucl. Fusion **55**, 093030 (2015).